

Article

Novel Voltage Control Method of the Primary Feeder by the Energy Storage System and Step Voltage Regulator

Byungki Kim ¹, Yang-Hyun Nam ¹, Heesang Ko ¹, Chul-Ho Park ¹ , Ho-Chan Kim ²,
Kyung-Sang Ryu ^{1,*}  and Dae-Jin Kim ^{1,*} 

¹ Jeju Global Research Center (JGRC), Korea Institute of Energy Research (KIER), 200 Haemajihae-an-ro, Gujwa-eup 63357, Jeju Specific Self-Governing Province, Korea

² Department of Electrical Engineering, Jeju National University, 102 Jejudaehak-ro, Jeju-si 63243, Jeju Special Self-Governing Province, Korea

* Correspondence: ksryu@kier.re.kr (K.-S.R.); djk@kier.re.kr (D.-J.K.);
Tel.: +82-64-800-2332 (K.-S.R.); +82-64-800-2225 (D.-J.K)

Received: 31 July 2019; Accepted: 28 August 2019; Published: 30 August 2019



Abstract: With the intention of keep the customer voltage within a nominal voltage boundary (the South Korea voltage regulation in range of 220 V \pm 6% for a single phase), the SVR (step voltage regulator) method in the primary feeder has been seriously systematized for the scheduled tap time delay (from a minimum of 120 s to a maximum of 900 s). The voltage must be compensated for the primary feeder during the tap delay time of SVR. However, when RES (renewable energy resource) is connected with the primary feeder, the customer voltage could exceed the nominal voltage boundary. Therefore, in order to keep the secondary feeder voltage within the nominal voltage boundary at all the time, this paper proposed a novel voltage control method in the primary feeder using coordinated controls between ESS (energy storage system) and SVR. Through the simulations based on PSCAD/EMTDC which is analysis tool of power system, it is confirmed that the proposed algorithm can effectively control the customer voltage within allowable limitation.

Keywords: step voltage regulator; coordinated control algorithm; energy storage system; PSCAD/EMDC; novel voltage control method

1. Introduction

As electrical power systems have been decentralized with the improvement of technology for renewable energy resource (RES), RES installs in the primary feeder. However, the secondary feeder, which has RES in the primary feeder, may cause various problems such as voltage variation, flicker, or harmonic, and so on [1]. In case of the electricity environment of South Korea, the voltage control of the secondary feeder must be 220 V \pm 6%.

Under the circumstance, the step voltage regulator (SVR), a voltage compensation device, is applied for voltage stabilization. SVR is also typically installed at the position of 10% voltage drop in the primary feeder, and it is operated by a line drop compensation method [2–4]. However, the operation time of a SVR is delayed from 120 to 900 s (named the scheduled delay time) due to mechanical characteristic of SVR. During the scheduled delay time, the customer voltage could not be maintained within the allowable limit. The references [5] and [2] dealt with contents to solve the feeder voltage problems using a LDC (line drop compensation) operation method that adjusts the sending voltage based on the increase and decrease of the load current, when a Photovoltaic (PV) system is interconnected with the primary feeder. However, the consumer voltage cannot maintain a nominal voltage boundary during the delay time of SVR tap operation. The methods for cooperative control using SVR, ULTC,

and SVC have also been proposed to solve the voltage problem caused by distributed power as shown in Table 1 [6–9]. In [10], a method for determining the installation position and tap position of the SVR is proposed considering the reverse power flow when the RES is connected with the distribution system as shown in Table 1. However, the operation time of a SVR is delayed from 120 to 900 s (named the scheduled delay time) due to the mechanical characteristic of SVR. During the scheduled delay time, the customer voltage could not be maintained within the allowable limit.

Table 1. Previous researches on voltage control of the distribution system.

Ref.	Contents
[6–8]	Cooperative control to adjust the voltage at the PCC using the SVR and reactive power of RES
[9]	Cooperative control scheme between ULTC, SVR, SC, SR, and SVC for voltage regulation of distribution system with RES
[10]	A method to determine the installation site and tap position of SVR in consideration of the reverse power flow of RES

To ensure the issue, the paper proposes an optimal voltage control method in the primary feeder using an energy storage system (ESS) and SVR, especially for all the time. To keep the customer voltage within the nominal voltage boundary during the delay time of SVR, ESS is operated as a discharging mode when the customer voltage is lower than 207 V or a charging mode when higher than 233 V. PSCAD/EMTDC was utilized to confirm the optimal voltage control method adapted in the operation strategy of SVR and ESS. In order to verify the novel voltage control method, this paper also performs voltage compensation characteristics of the proposed ESS control algorithm using the 30 kW scaled artificial distribution system simulator. From a systematical simulation analysis and test by the artificial test simulator, it shows that the customer voltage can be efficiently kept within the allowable limit.

2. Voltage Control of ESS Depending on the SVR Control Characteristic

Generally, the positions of SVR taps for sending voltage are decided by an LDC method and a reference tap (the nominal phase voltage of the primary feeder: 13,200 V). Then, the tap is changed by a tap operation decision in the voltage variation rate after the delay time. However, the voltage could easily be out of the nominal voltage boundary during the delay time due to the mechanical characteristic of the SVR as shown in Figure 1.

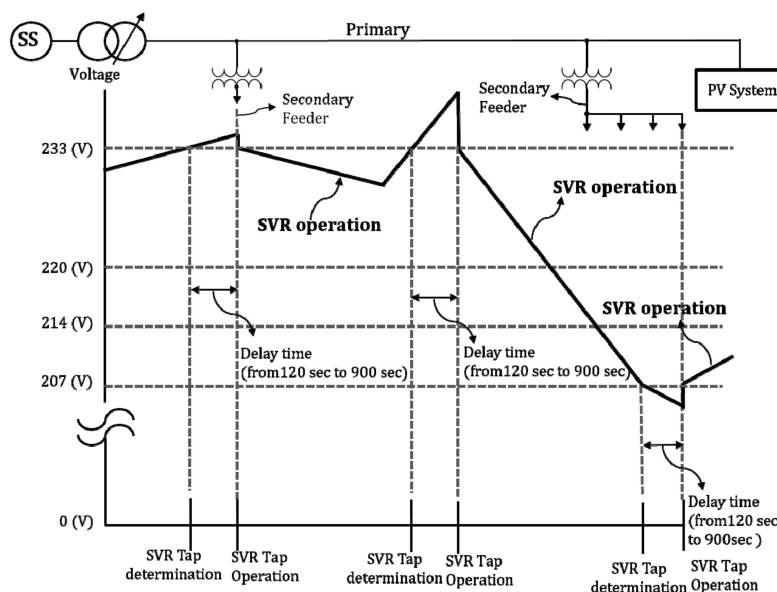


Figure 1. Voltage control in the primary feeder by the step voltage regulator (SVR).

In order to overcome the problem, ESS can compensate the voltage for the time delay of the SVR tap operation as shown in Figure 2. First of all, if the secondary feeder voltage is lower than the lower limit, ESS is discharged. When the secondary feeder voltage is also higher than the upper limit, ESS is charged. Therefore, ESS interception acts as the voltage stabilization during the time delay.

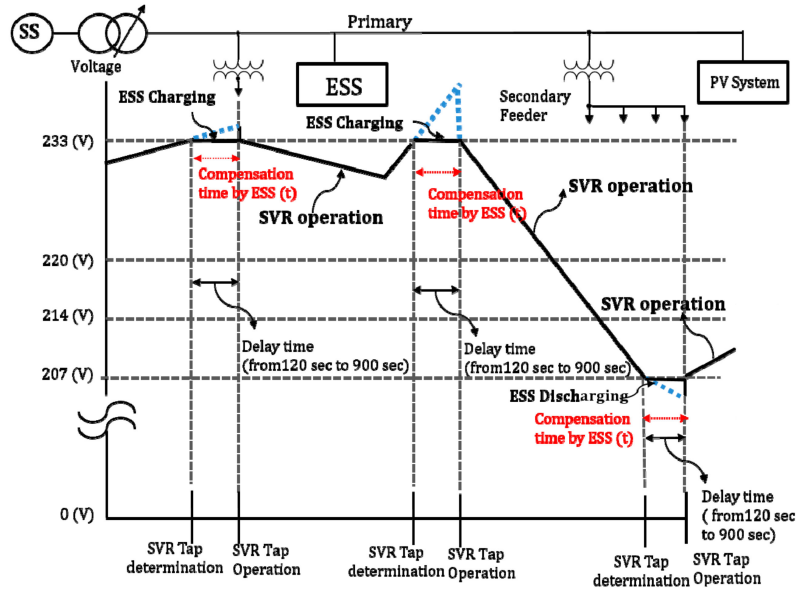


Figure 2. Voltage control of the SVR and energy storage system (ESS).

3. Modeling of the Primary Feeder with SVR and ESS

PSCAD/EMTDC was used to model grid systems with ESS, SVR, and RES (Figure 3). Herein, the primary and secondary feeders are composed of a total of six sections. RES is connected at the end section and ESS/SVR are located at the point of Section 3 in the primary feeder. Where, The pi (π) section model of Figure 3 is primarily used to represent a very short overhead transmission line. In other words, pi (π) sections provide a simplified means to represent transmission systems for steady state [11]. However, the capacitance value is not considered at the distribution power system model because of the section characteristic having a short length within 40 km.

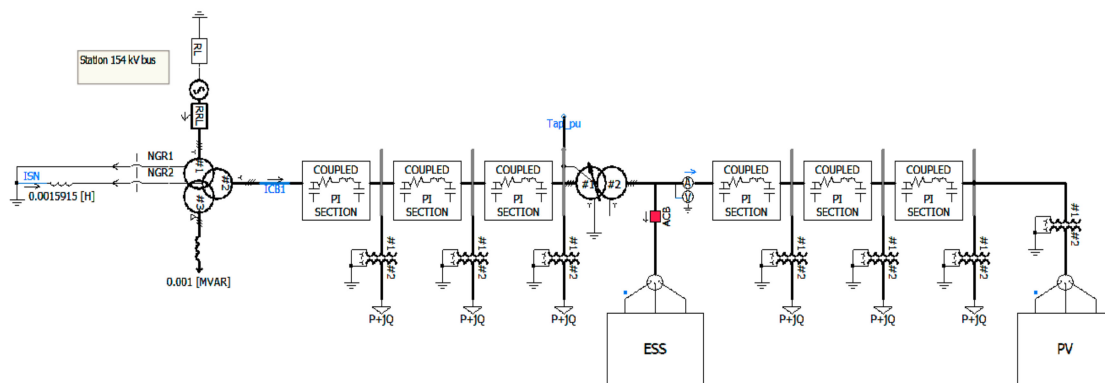


Figure 3. Distribution power system model.

3.1. Modeling of SVR

Decision for the optimal sending voltage of SVR is very important to build up modeling of SVR. Therefore, this paper tries for solving the optimal sending voltage setting values of the LDC method. The LDC method is statistically analyzed by comparing with ideal optimal sending voltages and total load currents (Figure 4).

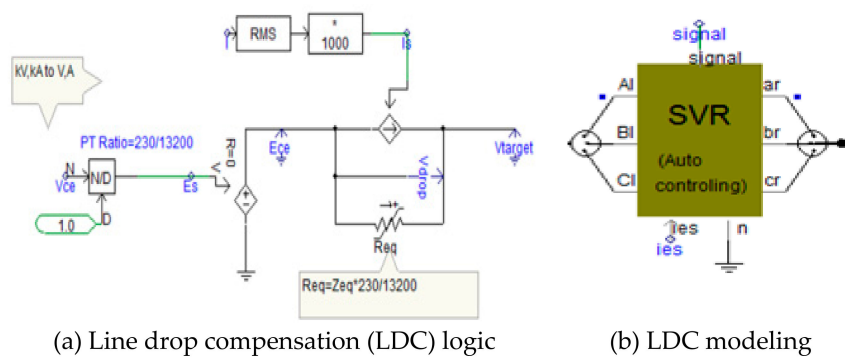


Figure 4. Line drop compensation (LDC) model of SVR.

Using the electrical modeling for the LDC method of SVR, the control logic is set in the range of the bandwidth of 50% and scheduled delay time of 120 s (Figure 5).

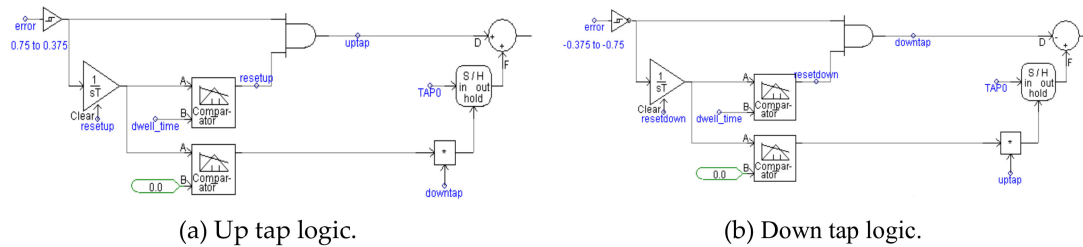


Figure 5. Tap up and tap down logic of SVR.

3.2. Modeling of ESS

ESS modeling is composed of a battery, a DC–DC converter, a bi-directional inverter, and a delta-wye transformer. Firstly, the battery model adjusts the parameters such as an initial SOC (state of charge), capacity, and C-rate. The battery is connected to the DC–DC converter. The DC–DC converter can determine the charging/discharging of the ESS based on the operation algorithm of ESS. It acts as a buck converter at charging, and as a boost converter at discharging (Figure 6).

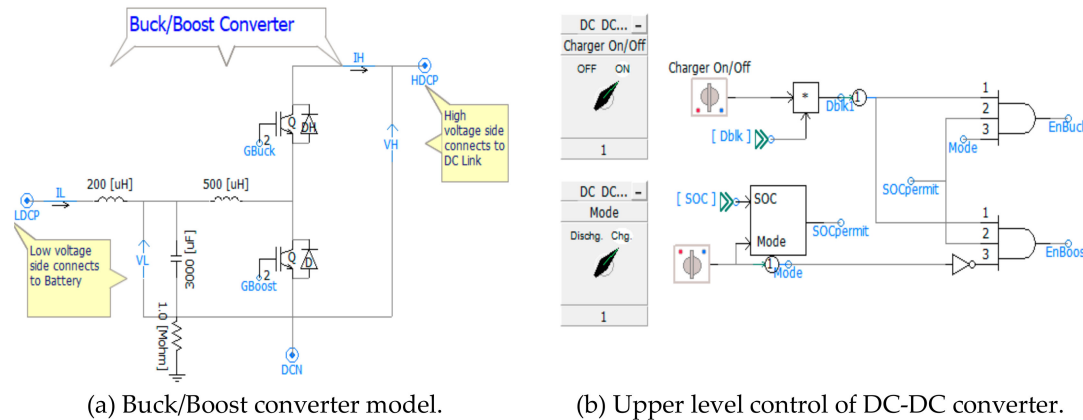


Figure 6. Model of ESS.

The output of the DC–DC converter is connected to the inverter through a DC-link, and the inverter controls the DC voltage on the DC-link and reactive power. The AC/DC conversions of voltage and current are also performed in the inverter and the output of the inverter is linked to the transformer [7]. The transformer converts the voltage level to the system and transfers power to the system. Figure 7 shows the overall configuration of an ESS consisting of the battery, the converter, then inverter, and the transformer.

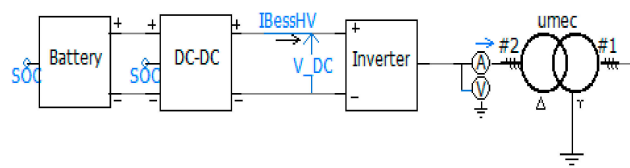


Figure 7. ESS model.

3.3. Modeling of PV

PV is modeled with a VSC (voltage source converter) and a current source, and the solar power is replaced by a current source as shown in Figure 8a. The current source linearly depends on the power. The control strategy is presented in Figure 8b. The voltage and current of the grid are decomposed into a direct component and a quadrature component through a Park transform and PLL (phase locked loop). The direct component of current I_d regulates the active power, and the quadrature component of current I_q controls the reactive power. On the other hand, the six pulse waveforms for driving the IGBT (insulated gate bipolar transistor) are obtained by the inverse Park transform of I_d , I_q , and set point values of V_d and V_q .

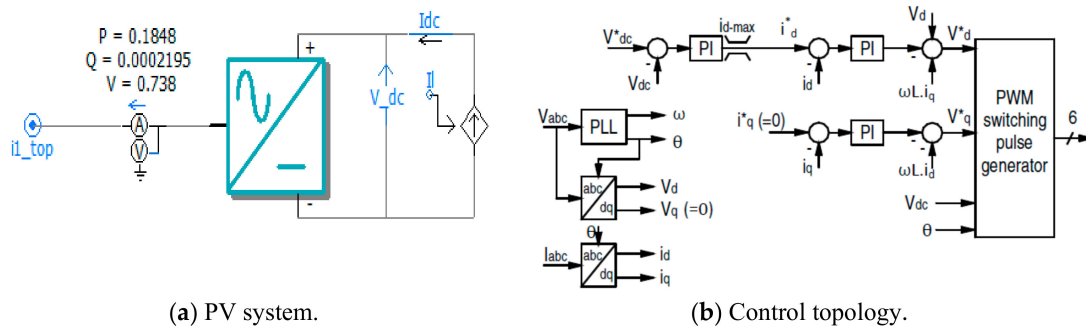


Figure 8. Photovoltaic system model.

4. Novel Voltage Control Method of SVR and ESS

4.1. SVR Control Algorithm

The LDC method of SVR, which is installed at the primary feeder to compensate the voltage variations, finds the optimal setting values (V_{ce} , Z_{eq}) and optimal sending voltages ($V_{send}(t)$) in order to deliver suitable voltages to as many customers as possible. Firstly, the LDC method determines the ideal optimal sending voltages, which can be expressed by the optimal compensation rates of SVR, and then obtains optimal setting values by statistical analysis according to the relationship between ideal optimal sending voltages and total load currents [3,12,13]. Optimal sending voltages have a general relationship with LDC setting values as shown in Equation (1). Therefore, the optimal setting values can be calculated by solving the equation for V_{ce} and Z_{eq} [3,4].

$$V_{send}(t) = V_{ce} + Z_{eq} \times I_{load}(t). \quad (1)$$

In addition, in order to curb the increment for introduction capacity of ESS, this paper proposed an improved method to determine optimal sending voltage of SVR by the comparison of measured ESS and load current from the Equation (1) and Figure 9 as: The positive (+) signal of ESS operation ($I_{ESS.ct}$) means the discharging mode and negative (-) signal ($I_{ESS.ct}$) means the charging mode.

$$V'_{send}(t) = V_{ce} + Z_{eq} \times (I_{load} \pm I_{ESS.ct})(t), \quad (2)$$

where, $V'_{send}(t)$ is the optimal sending voltage of SVR based on I_{load} and $I_{ESS.ct}$, and $I_{ESS.ct}(t)$ is the measured current value of ESS.

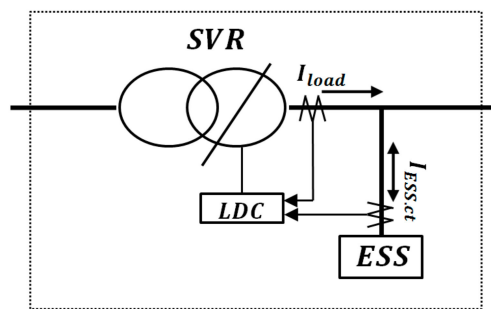


Figure 9. Concept for the proposed current measuring method of SVR and ESS.

In other words, $I_{load} \pm I_{ESS.ct}$ is the passing current of SVR, which does not consider the measured current of ESS ($I_{ESS.ct}(t)$) when ESS is operated during the delay time.

As mentioned earlier, the tap decision of SVR is considered by the compensation rate from the relationship between the sending voltage ($V_{send}'(t)$) for the LDC method and reference tap (13,200 V) of SVR, and then the tap should be operated when it is violated to the bandwidth (50%) during the time delay (from a minimum of 120 s to a maximum of 900 s) as shown in Figure 10. The left box (①) is the SVR control part by input of the LDC method including the measuring element and predetermined, V_{ce} and Z_{eq} . The right box (②) in Figure 10 means the SVR operation part to control the SVR tap. The tap operation procedure is performed as below.

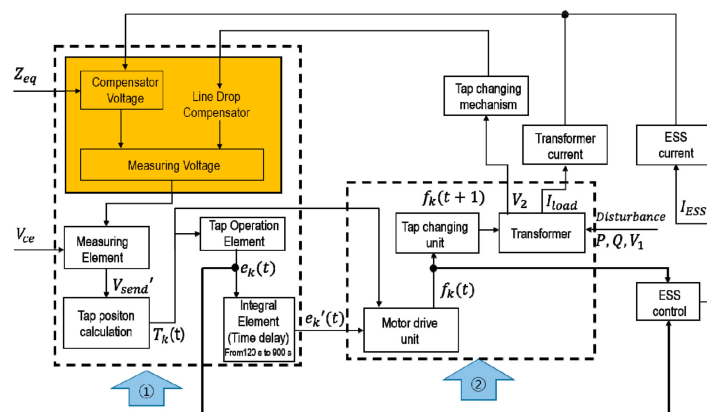


Figure 10. Operation block diagram of SVR.

First of all, based on the above LDC determination of SVR, the tap position ($T_k(t)$) of SVR will be calculated by the optimal sending voltage, reference voltage of SVR (13,200 V), and tap interval of SVR (0.0125) for coordinated operation between SVR and ESS as shown in Figure 3. The tap position, as an integer value, is also not rounded when the decimal point is 0.5 or less. Here, the tap position of SVR means the tap down condition when $T_k(t)$ is (+) value and the tap position of SVR means the tap up condition when $T_k(t)$ is (-) value.

$$\text{int } T_k(t) = \frac{V_{send}'(t) - V_{svr}}{V_{svr} \times \text{Tap}_{int}}, \quad (3)$$

where, $T_k(t)$ is the desired tap position of SVR, $V_{send}'(t)$ is the optimal sending voltage of SVR based on I_{load} and $I_{ESS.ct}$, $V_{svr}(t)$ is the reference voltage of SVR(13,200 V), and Tap_{int} is the tap interval of SVR (1.25%).

Based on the tap position ($T_k(t)$), the tap operation signal ($e_k(t)$) of the SVR is determined by comparing between the calculated SVR tap positions (T_k) and the existing SVR tap position ($T_{k\text{ SVR}}$) expressed in Equation (4). The tap operation signal $e_k(t)$ is adapted by the voltage control algorithm of

chapter 4.2 to operate ESS only for the delay time of SVR. The value of tap operation signal ($e_k(t)$) has “1” or “0” at the operation and non-operation states, respectively.

$$e_k(t) = \left\{ \begin{array}{l} 1 \text{ if } |T_k|t - T_{k\text{ SVR}} \neq 0 \\ 0 \text{ otherwise} \end{array} \right\}, \tag{4}$$

where, $e_k(t)$ is the tap operation signal of SVR, and $T_{k\text{ SVR}}$ is the existing tap location of SVR.

Finally, SVR is operated after a time delay (TP sec) when the integral value ($e_{k'}(t)$) of the tap operation signal ($e_k(t)$) is bigger than 70% of the time delay (TP) in Equation (5). Measuring the time unit of the signal ($e_k(t)$) means 1 s. The SVR tap is operated by the integral value of the tap operation signal and tap determination value ($f_k(t)$) when the ($e_{k'}(t)$) value becomes the “1” signal as indicated in Equation (6).

$$e_{k'}(t) = \left\{ \begin{array}{l} 1 \text{ if } \int_{t_0}^{t_{\text{delay}}} e_k\{t\} > TP \times 0.7 \\ 0 \text{ otherwise} \end{array} \right\}. \tag{5}$$

Subject to $t_{\text{delay}}(t) = TP$, It means time interval of SVR operation from minimum 120 s to maximum 900 s.

$$f_k(t) = e_{k'}(t) \times T_k(t), \tag{6}$$

where, $e_{k'}(t)$ is the integral value of the tap operation signal considering time delay, $f_k(t)$ is the tap position determination value, and $t_{\text{delay}}(t)$ is the time delay of SVR (from 120 s to 900 s).

4.2. Novel Voltage Control Algorithm of ESS

4.2.1. Operation determination of ESS

Operation block diagram of ESS using the SVR control mode is shown in Figure 11. At first, operation of ESS ($\sigma(t)$) is determined by the tap operation signal of SVR and the operation reference value of ESS when the customer voltage is violated to the nominal voltage boundary (220 ± 13 V). Then, the voltage compensation rate ($E_{\text{oper}}(t)$: Voltage control range) is calculated by the relationship between the operation reference values of ESS and customer voltages (measuring at P.tr location) in real time. After that, the operation capacity (charging or discharging) of ESS should be recalculated by the sum of the impedances from the substation to ESS installation section and the voltage control range of the ESS. Finally, ESS is only operated by the SVR tap and ESS signals during the delay time (120 s). If the customer voltage is satisfied in the nominal voltage boundary during the operation of SVR tap, ESS should be not operated during the operation signal of ESS ($\sigma(t)$).

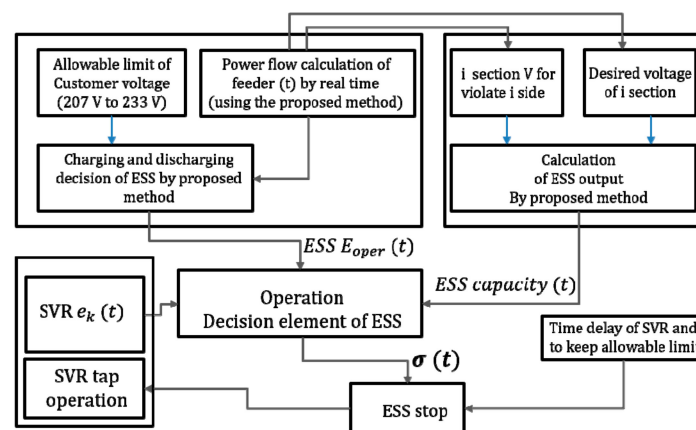


Figure 11. Operation block diagram of ESS.

However, it is difficult to identify the voltage of multiple customers in the distribution system. Therefore, this paper proposed a method of calculating the customer voltage that cannot maintain the allowable limitation. Equations (7) and (8) are a problem of the estimating real-time customer voltage [14]. It is determined by the voltage ($V_{c,i}(t)$) profile of the primary feeder the calculating Gauss–Seidel method, tap voltage of the pole transformer, voltage drop rate of the secondary feeder, and the load factor before operation of ESS.

$$V_{customer_{d,i}}(t)[V] = \left((V_{c,i}(t)) \times \frac{V_{ptr_{2nd}}}{V_{ptr_{1st}}} \right) - V_d \times f_h, \quad (7)$$

$$V_{customer_{e,i}}(t)[V] = \left((V_{c,i}(t)) \times \frac{V_{ptr_{2nd}}}{V_{ptr_{1st}}} \right) - V_e \times f_h, \quad (8)$$

where, $V_{customer_{d,i}}$ is the first customer voltage in the secondary feeder at i section, $V_{customer_{e,i}}$ is the last customer voltage in the secondary feeder at i section, i is the section number in the primary feeder, $V_{c,i}(t)$ is the i section voltage of the primary feeder calculating the Gauss–Seidel method, $V_{ptr_{2nd}}$ is the secondary turn ratio of pole transformer, $V_{ptr_{1st}}$ is the primary turn ratio of the pole transformer, V_d is the voltage drop rate from the pole transformer to first customer of the secondary feeder, V_e is the voltage drop rate from the pole transformer to the last customer of the secondary feeder, and f_h is the load factor of the secondary feeder.

Based on the calculated customer voltage in Equations (7) and (8) earlier, the ESS operation in Equation (9) is recognized as a charging mode ($E_{deter}(t) = -1$) when the customer voltage is exceeded then the upper limit value (233 V) and the discharging mode ($E_{deter}(t) = 1$) is performed when the voltage is kept below the lower limit (207 V). In order to operate the ESS, it is assumed that the first and the last customer voltages of the secondary feeder terminal can be checked in real time by the measuring device.

$$E_{deter}(t) = \begin{cases} -1 & \text{if } V_{customer_{d,i}} \text{ or } V_{customer_{e,i}} \geq 233V \\ 1, & \text{if } V_{customer_{d,i}} \text{ or } V_{customer_{e,i}} \leq 207V \\ 0, & \text{otherwise} \end{cases}, \quad (9)$$

where, E_{deter} is the determination signal for charging and discharging of ESS.

Under the concept, a modified equation for the operation of the ESS is expressed in Equation (10). Specifically, in order to operate only the time delay of the SVR tap, the final operation signal of ESS is released by the relationship between the tap operation signal of SVR and the decision signal of ESS from Equation (4). Here, ESS should be operated only when the customer voltage violates the allowable limit during the delay time of SVR.

$$\sigma(t) = E_{deter}(t) \times e_k(t), \quad (10)$$

where, $\sigma(t)$ is the operation signal for charging and discharging of ESS in order to operate the time delay of the SVR tap.

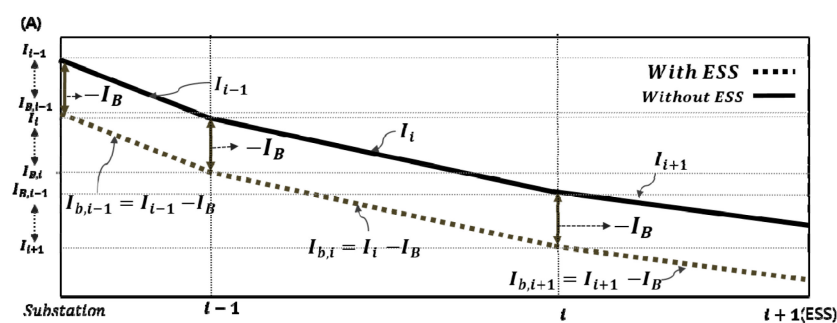
4.2.2. Determination for the Operation Capacity of ESS

Based on the operation determination of ESS, the decision problem for the voltage control range is defined as follows. When the operation of the ESS is decided, the voltage control range ($E_{oper}(t)$) to maintain the allowable limit for the customer voltage is calculated as shown in Equation (11). In other words, when operation of ESS is determined, the voltage control range is calculated by the difference between the maximum voltage (measuring pole transformer location) or minimum voltage in real time of the primary feeder and limit values (upper and lower limit). Here, the upper limit means a converted primary voltage to setting value ($V_{char}(t)$) for ESS charging and the lower limit means a converted primary voltage to setting value ($V_{dis}(t)$) for ESS discharging.

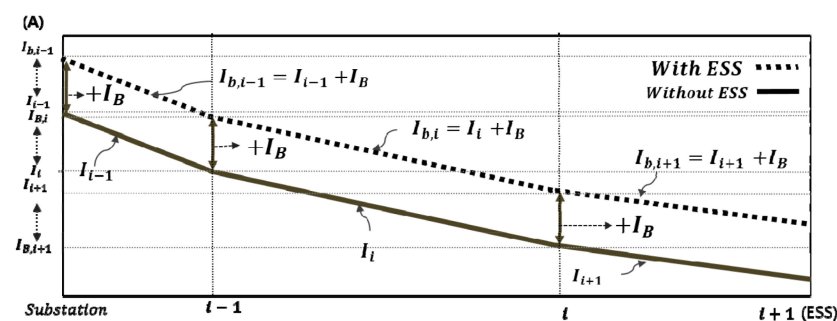
$$E_{oper}(t) = \begin{cases} |Max V_{c.i}\{t - V_{char} t\}|, & \text{if } \sigma\{t = -1 \\ |Min V_{c.i}\{t - V_{dis} t\}|, & \text{if } \sigma\{t = 1 \\ claculation, & \text{otherwise} \end{cases} \quad (11)$$

where, $E_{oper}(t)$ is the voltage control range of ESS, $Max V_{c.i}$ is the maximum voltage of primary feeder in real, $Min V_{c.i}$ is the minimum voltage of primary feeder in real time, $V_{char}(t)$ is the setting value for charging of ESS, and $V_{dis}(t)$ is the setting value for discharging of ESS.

Therefore, voltage compensation by ESS is based on the principle of the following grid voltage characteristics. The load current of each section by the operation of the ESS decreases (ESS discharging) or increases (ESS charging) in the operating current of the ESS as shown in Figure 12. At this time, the primary feeder voltages are dropped or raised by the relationship between fixed impedance and the amount of current at the prior sections of an ESS site.



(a) Current characteristic in the grid in case of the ESS charging mode.



(b) Current characteristic in the grid in case of the ESS discharging mode.

Figure 12. Current characteristic in the grid according to the ESS operation.

The operation capacity of the ESS as shown in Equation (12) is determined by the sum of the impedances from the substation to ESS installation section and the voltage control range of the ESS in Equation (11). However, the operating current of the ESS has constraint to be kept within 50% of the maximum rated current of the primary feeder (standard: 22.9 kV, 10 MVA feeder) because SVR is installed at the section of the 615 V voltage drop.

$$S_{ESS}[VA](t) = \frac{E_{oper}(t)}{\sum_{i=1}^{nb} R_i + j \sum_{i=1}^{nb} X_i} \times V_{ESS}(t), \quad (12)$$

$$Subj. \text{ to } \frac{\text{Primary feeder [A]}}{2} > I_B = \frac{E_{oper}(t)}{\sum_{i=1}^{nb} R_i + j \sum_{i=1}^{nb} X_i},$$

where, S_{ESS} is the ESS operation capacity, I_B is the ESS operation current, $V_{ESS}(t)$ is the section voltage at ESS installation site (V), i is the section number R_i , and X_i is the total line impedance (resistance and reactance) from substation to i th, and nb is the number for the installation section of ESS

4.3. Voltage Control Algorithm Between SVR and ESS

As mentioned the operation procedure for SVR and ESS according to the Equations (3) to (12), the study proposed the voltage control algorithm between SVR and ESS as shown in Figure 13. The tap of SVR should be operated by the LDC method when a voltage problem like voltage fluctuation is revealed at the distribution system. In this case, the tap is operated after the delay time. Therefore, for the allowable customer voltage, ESS is operated as the charging mode when the customer voltage should be lower than 207 V, or the discharge mode when customer voltage should be higher than 213 V.

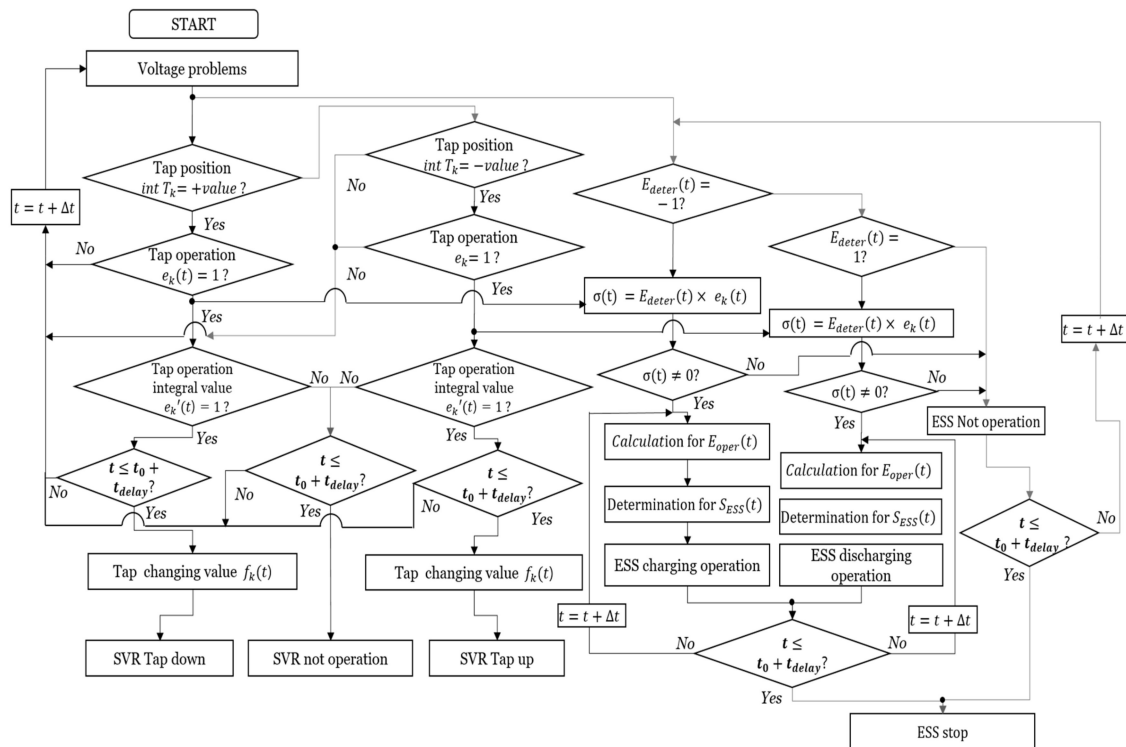


Figure 13. Voltage control algorithm by SVR and ESS.

5. Case Studies

5.1. Simulation Conditions

Based on the model of the primary feeder in Figure 14, the distribution parameter and section data of the primary feeder are assumed as Table 2. Pole transformer (P.tr) is considered as 13,200 V/230 V. Voltage drops at the first and last customers of the secondary feeder are considered in rated voltages of 2% and 8% (220 V).

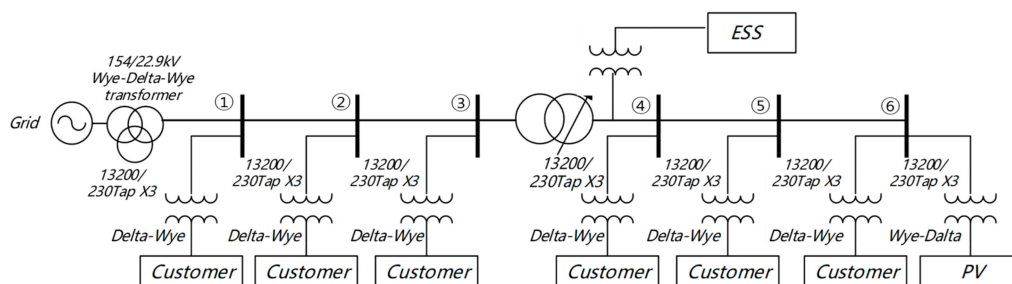
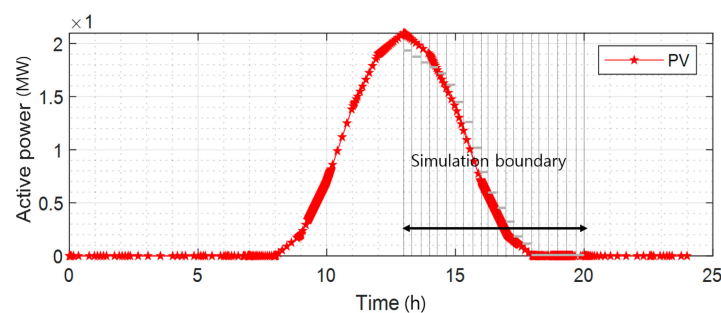


Figure 14. Voltage control algorithm by SVR and ESS.

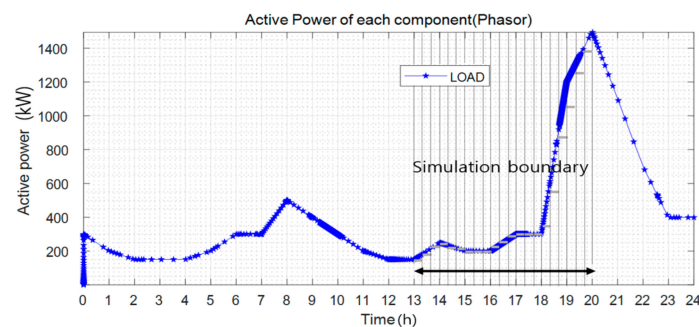
Table 2. Simulation Data.

Section Number	Impedance		Length (km)	Power Factor	Load (MW)	PV System (MW)
	R (Ω /km)	X (Ω /km)				
1	0.182	0.391	3	0.9	0.2–0.8	0
2	0.182	0.391	4	0.9	0.2–0.8	0
3	0.182	0.391	3	0.9	0.2–0.4	0
4	0.182	0.391	10	0.9	0.6–1.6	0
5	0.182	0.391	8	0.9	0.8–1.8	0
6	0.182	0.391	3	0.9	0.4–2.0	0–1.9

The load pattern and output of RES with the PV system is also predicted as shown in Figure 15. The load and PV patterns are simulated by the operation characteristics of SVR in the delay time of 15 min. The simulation boundary is divided into 21 steps during 7 h (step means 20 min).



(a) Load characteristic of customer side.

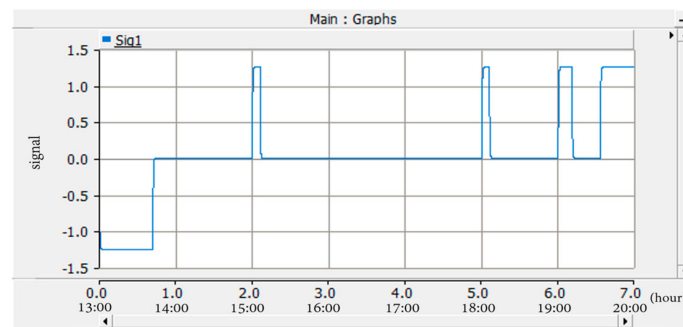
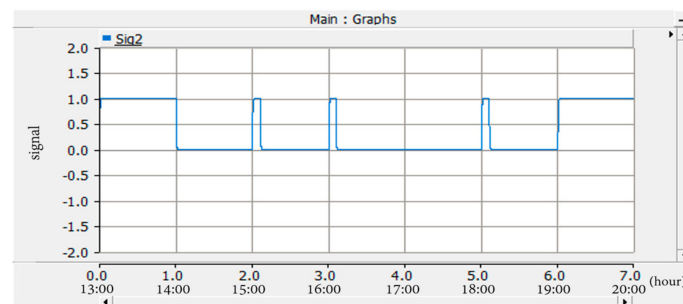
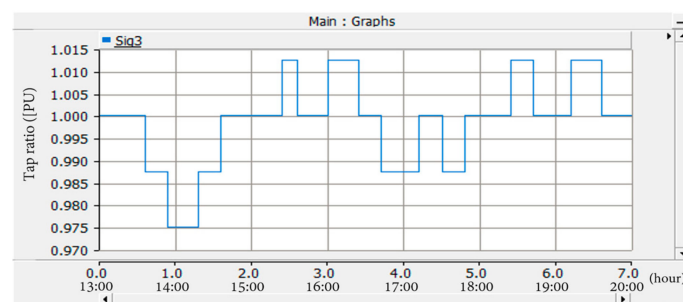


(b) Output characteristic of PV system.

Figure 15. Output pattern of the PV system and customer.

5.2. Verification for the Operation Strategy of ESS and SVR

To verify simulation results for the voltage customer voltage characteristic in the secondary feeder for SVR and ESS, the operating characteristics of the ESS should be confirmed at lower than 233 V or higher than 207 V. The operating time of the ESS was from 13:00 to 20:00, considering the output pattern of the RES (the PV system). When the customer voltage was not kept at an allowable limit, ESS can be operated during the only time delay of SVR by the operation signal of ESS ($\sigma(t)$) in Figure 16a by the determination signal of ESS ($E_{deter}(t)$) as shown in Figure 16b and tap operation signal of SVR ($e_k(t)$) expressed in Figure 16c. Therefore, it was clear that the voltage control method of ESS/SVR was efficiently worked.

(a) Charging and discharging operation signal of ESS ($\sigma(t)$).(b) Determination signal of ESS ($E_{deter}(t)$)(c) Tap operation signal of SVR ($e_k(t)$)**Figure 16.** Operation characteristic by the control modeling of ESS.

5.3. Analysis of the Customer Voltage Characteristic by ESS and SVR Operation

Figures 17 and 18 show the customer voltage characteristics of the secondary feeder from Section 4 to the end section in the primary feeder interconnected with RES. The customer voltage was analyzed from 13:00 to 20:00 per hour based on the output pattern of RES and the load pattern as shown in Figures 14 and 15. The result of the simulation reveals that the customer voltage could not be maintained to reasonable conditions (over voltage phenomena) at Section 6 when the PV system generated the maximum output at 13:00–14:00 as shown in Figure 17. At 19:00–20:00 the customer voltage was also lower than the limit of 207 V at Section 6 due to power demands of customers as shown in Figure 18. Meanwhile, the customer voltage could not exactly be kept within the nominal voltage boundary because the voltage was not compensated during the delay time of SVR.

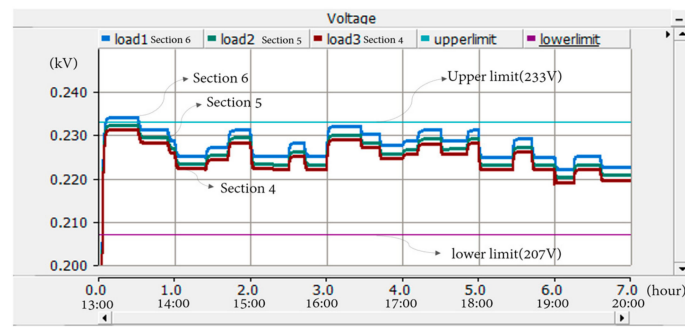


Figure 17. Analysis of the customer voltage characteristic by SVR operation (upper limit).

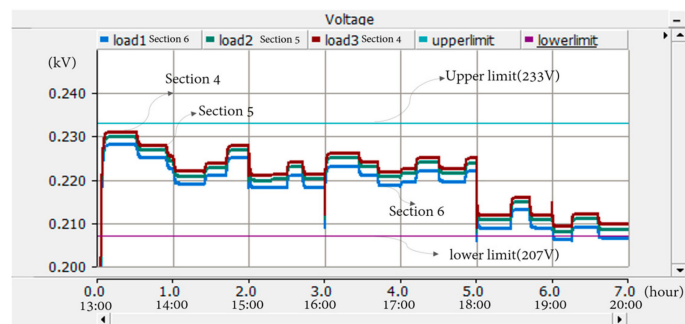


Figure 18. Analysis of the customer voltage characteristic by SVR operation (lower limit).

Figures 19 and 20 show the customer voltage characteristic of the secondary feeder from Section 4 end in the primary feeder connected with RES. SVR/ESS were also located at Section 3. As the result of the simulation, all of the customer voltages at Section 6 could be exactly maintained within the allowable limits according to the voltage control method of SVR and ESS. In other words, over voltage (from 13:00 to 14:00) and low voltage (from 19:00 to 20:00) during the delay time of SVR were solved by ESS operation as shown in Figures 19 and 20. Therefore, the coordinated operation of SVR/ESS could make the customer voltage of the distribution system with the PV system keep better voltage conditions. However, the voltage data showed some variation characteristics within tolerance by the converter operation for ESS.

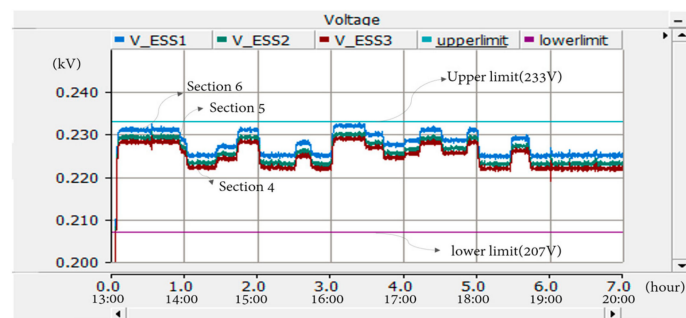


Figure 19. Analysis of the customer voltage characteristic by ESS and SVR operation (upper limit).

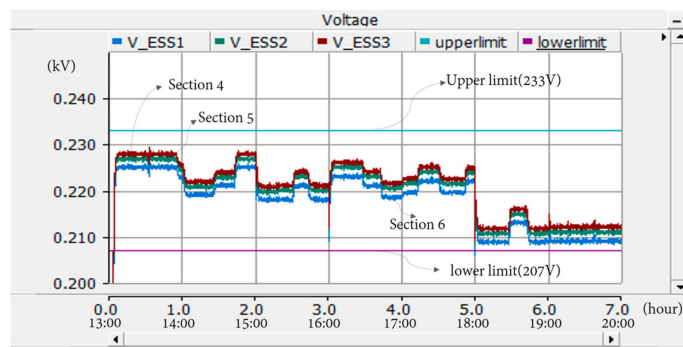
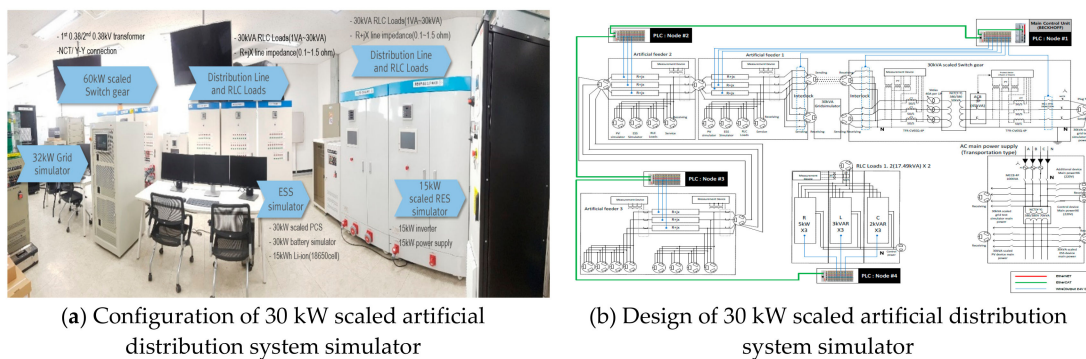


Figure 20. Analysis of the customer voltage characteristic by ESS and SVR operation (lower limit).

5.4. Verification of the Present Method by a Real Simulator

In order to verify the novel voltage control method, this paper performed voltage compensation characteristics of the proposed ESS control algorithm using the 30 kW scaled artificial distribution system simulator as shown in Figure 21. The artificial distribution system simulator is composed of the distribution system, PV system (inverter, DC power supply), ESS system (power conditioning system, Li-ion (18650 cell), battery simulator), grid-simulator, and switch gear (protection devices, controller devices). It is also adapted as a pre-test for the present method to solve the distribution system problems (steady state, power quality, etc.). However, the characteristics of the SVR are not implemented in this simulator. Therefore, it was assumed that the operation signal of the SVR was generated, before characteristics of the available voltage by ESS operation were analyzed.



(a) Configuration of 30 kW scaled artificial distribution system simulator

(b) Design of 30 kW scaled artificial distribution system simulator

Figure 21. Configuration of 30 kW scaled artificial distribution system simulator.

On the other hand, the test parameter and configuration of the simulator were assumed as Table 3 and Figure 22.

Table 3. Test condition.

Classification	Low Voltage Condition			Over Voltage Condition		
	R	S	T	R	S	T
Load (3 phase)	8 kW			3 kW		
Line impedance (ohm)	1.0 + j0.2 Ω			1.0 + j0.2 Ω		
Customer voltage (V)	218.9	220.5	222.7	219.2	220.6	223.0
RES output (kW)	-			10 kW		

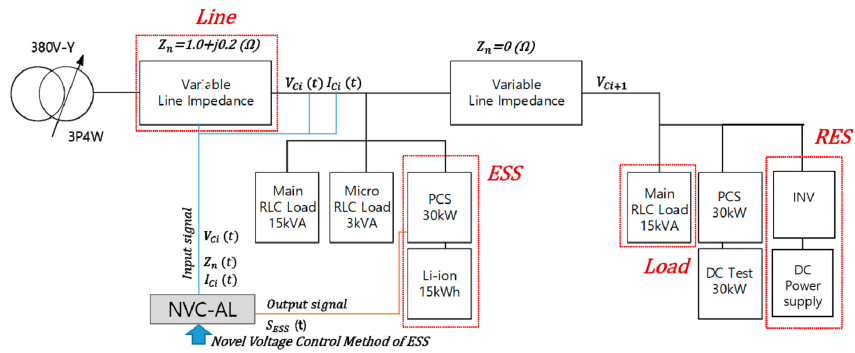


Figure 22. Test configuration.

Figure 23 shows the customer voltage characteristic only introduced RES and load, assuming a time delay before the SVR operation. From the test results according to the test conditions of two cases (low voltage condition, over voltage condition), it was confirmed that customer voltage could not be maintained to reasonable conditions (low voltage phenomena (R: 205.6V, S: 204.2 V, T: 203.4 V) and over voltage phenomena (R: 232.7 V, S: 232.9 V, T: 233.1 V)) during the time delay of SVR tap operation above simulation results by the PSCAD/EMTDC.

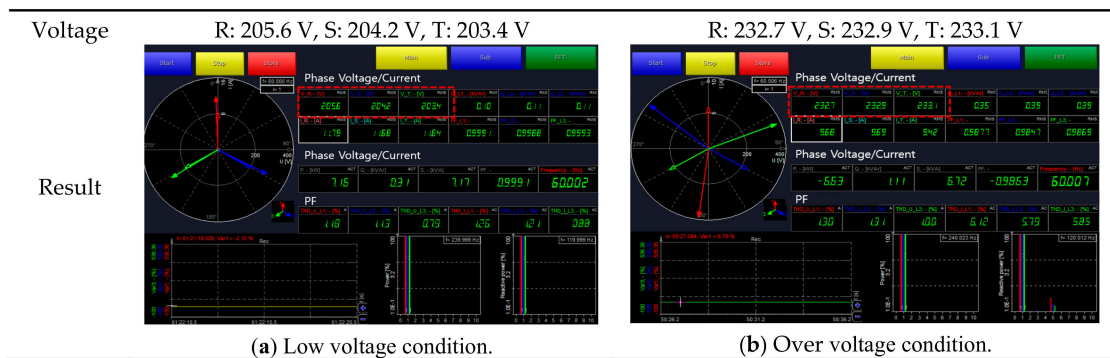


Figure 23. Test results of the customer voltage characteristic by only SVR (assumed) operation.

On the other hands, Figure 24 shows the customer voltage characteristic by the voltage control of ESS when it is interconnected with RES and load and assuming a time delay before the SVR operation. In order to analyze operation characteristic of ESS accurately, objective compensation voltage level by the ESS was also set as 6 V. As the result of the artificial test, customer voltages were exactly maintained within the allowable limits according to the voltage control method of ESS above simulation results by the PSCAD/EMTDC. Therefore, the present method was verified that voltage compensation though the coordination control between SVR and ESS could be possible.

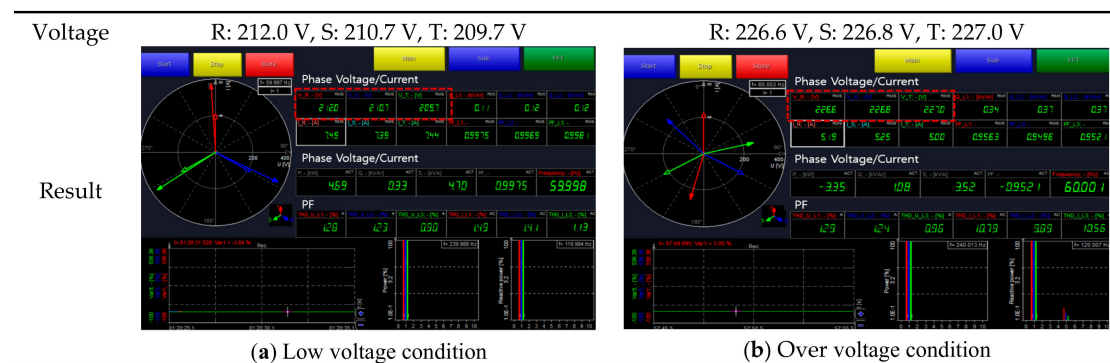


Figure 24. Test results of the customer voltage characteristic by ESS and SVR (assumed) operation.

6. Discussion

The characteristic of customer voltage distributions can be evaluated by the degree of how close customer voltages are maintained to the nominal voltage. Therefore, a performance index can be defined as a form of the squared differences between the nominal voltage and customer voltages of all nodes as follows:

$$PI(t) = \sum_{t=1}^T \sum_{i=1}^N [\{V_{customer_d}(t, i) - V_r\}^2 + \{V_r - V_{customer_e}(t, i)\}^2]. \quad (13)$$

$V_{customer_d}$ is the first customer voltage in the secondary feeder at i section, $V_{customer_e}$ is the last customer voltage in the secondary feeder at i section, V_r is the reference voltage (220 V), T is the total operation time, and N is the total amount of the section.

Figure 25 and Table 3 show the performance index by the introduction of SVR and ESS in distribution system with renewable energy sources. From the result of the performance index based on Table 4, it was clear that the coordinated customer voltage kept better within the nominal voltage boundary by the operation method between SVR and ESS than only the operation of ESS.



Figure 25. Comparison of the performance index for simulation results.

Table 4. Comparison of the performance index of each method.

	Only SVR Operation	SVR and ESS Operation
Performance index value	10665.26	9735.55

7. Conclusions

The paper proposed the modeling of SVR/ESS based on the PSCAD/EMTDC and the optimal coordinated control method of SVR/ESS in the primary feeder connected with the RES. The main results are summarized as follows:

- (1) In order to overcome voltage problems, the voltage control method using operating ESS during the time delay of SVR tap operation was proposed. First of all, if the secondary feeder voltages dropped below the lower limit, ESS was working at a discharging state. When the secondary feeder voltage was higher than the upper limit, ESS was operated as a charging state. As mentioned earlier, the role of ESS as a voltage stabilization function was kept within the nominal voltage boundary at the secondary feeder voltage during the time delay (from the 120 s to 900 s) of the SVR tap.
- (2) The simulation results stated that the customer voltage could not be maintained in reasonable conditions (over voltage phenomena) when the PV system generated in the maximum during the delay time of SVR. It was found that the customer voltage was lower than the limit of 207 V caused by power demands of customers. Therefore, it was clear that the customer voltage could not be exactly kept within the nominal voltage boundary because the voltage was not compensated during the delay time of SVR.

- (3) From the simulation results of SVR/ESS, it was clear that the customer voltage could be sustained in reasonable conditions. Meanwhile, the ESS operation could solve the over and under voltage during the delay time of SVR. The customer voltage could be exactly maintained within the nominal voltage boundary according to the operation of ESS during the time delay of SVR.

Author Contributions: All of the authors contributed to publishing this paper. B.K. carried out modeling, simulations and compiled the manuscript. The literature review and simulation analysis were performed by D.J.K., K.S.R., H.C.K., C.H.P., H.K., and Y.H.N. collected the data and investigated early works.

Funding: This research was funded by the [Ministry of Trade, Industry and Energy, and supported by the Korea Institute of Energy Technology Evaluation and Planning (KETEP)] grant number [No. 20172410100030]. This work was conducted under the framework of Research and Development Program of the Korea Institute of Energy Research (KIER) (No. B9-2421). The APC was funded by [No.20172410100030].

Acknowledgments: This research was funded by the Ministry of Trade, Industry and Energy, and supported by the Korea Institute of Energy Technology Evaluation and Planning (KETEP) (No. 20172410100030). This work was conducted under the framework of Research and Development Program of the Korea Institute of Energy Research (KIER) (No. B9-2421).

Conflicts of Interest: The authors declare no conflict of interest.

References

- Rho, D.-S.; Kook, K.-S.; Wang, Y.-P. Optimal Algorithms for Voltage Management in Distribution Systems Interconnected with New Dispersed Sources. *J. Electr. Eng. Technol.* **2011**, *6*, 192–201. [[CrossRef](#)]
- Kim, B.; Kim, G.; Lee, J.; Choi, S.; Rho, D. A Study on the Modeling of Step Voltage Regulator and Energy Storage System in Distribution System Using the PSCAD/EMTDC. *J. Korea Acad.-Ind. Coop. Soc.* **2015**, *16*, 1355–1363.
- Kim, M.; Hara, R.; Kita, H. Design of the Optimal ULTC Parameters in Distribution System with Distributed Generations. *IEEE Trans. Power Syst.* **2009**, *24*, 297–305.
- Rho, D.; Lee, E.; Choi, J.; Kim, J.; Kim, E.; Park, C. A study on the Optimal Operation of Line Voltage Regulator (SVR) in Distribution Feeders. *IFAC Proc. Vol.* **2003**, *36*, 535–539. [[CrossRef](#)]
- Kim, B.K.; Choi, S.S.; Wang, Y.P.; Kim, E.S.; Rho, D.S. A Study on the Control Method of Customer Voltage Variation in Distribution System with PV Systems. *J. Electr. Eng. Technol.* **2014**, *10*, 838–846. [[CrossRef](#)]
- Farag, H.E.; El-Saadany, E.F. Voltage Regulation in Distribution Feeders with High DG Penetration: From Traditional to Smart. In Proceedings of the 2011 IEEE Power and Energy Society General Meeting, Detroit, MI, USA, 24–28 July 2011; IEEE: Piscataway, NJ, USA, 2011; pp. 1–8.
- Kojovic, L.A. Modern techniques to study voltage regulator-DG interactions in distribution systems. In Proceedings of the 2008 IEEE/PES Transmission and Distribution Conference and Exposition, Chicago, IL, USA, 21–24 April 2008; IEEE: Piscataway, NJ, USA, 2008; pp. 1–6.
- Kojovic, L.A. Coordination of distributed generation and step voltage regulator operations for improved distribution system voltage regulation. In Proceedings of the 2006 IEEE Power Engineering Society General Meeting, Montreal, QC, Canada, 18–22 June 2006.
- Senjyu, T.; Miyazato, Y.; Yona, A.; Urasaki, N.; Funabashi, T. Optimal distribution voltage control and coordination with distributed generation. *IEEE Trans. Power Deliv.* **2008**, *23*, 1236–1242. [[CrossRef](#)]
- Sugimoto, J.; Yokoyama, R.; Fujita, G.; Fukuyama, Y. Cooperative Allocation of SVR and SVC for Voltage Fluctuation in Case of Connecting Distributed Generators. *IEEE Trans. Power Energy* **2006**, *126*, 1191–1198. [[CrossRef](#)]
- PSCAD/EMTDC. Three-Phase Battery Energy Storage System; Reversion 1; Powered by Manitoba Hydro International Ltd., Canada. Available online: <https://hvdc.ca/engineering/> (accessed on 29 August 2019).
- Kim, C.; Park, O.; Lee, B.; Rho, D. Optimal algorithms for voltage management in distribution systems interconnected with new dispersed sources. In Proceedings of the 2009 Transmission & Distribution Conference & Exposition: Asia and Pacific, Seoul, Korea, 26–30 October 2009; IEEE: Piscataway, NJ, USA, 2009; pp. 1–4.

13. Takahashi, S.; Hayashi, Y.; Tsuji, M.; Kamiya, E. Method of optimal allocation of svr in distribution feeders with renewable energy sources. *J. Int. Council Electr. Eng.* **2012**, *2*, 159–165. [[CrossRef](#)]
14. Liu, X.; Aichhorn, A.; Liu, L.; Li, H. Coordinated control of distributed energy storage system with tap changer transformers for voltage rise mitigation under high photovoltaic penetration. *IEEE Trans. Smart Grid* **2012**, *3*, 897–906. [[CrossRef](#)]



© 2019 by the authors. Licensee MDPI, Basel, Switzerland. This article is an open access article distributed under the terms and conditions of the Creative Commons Attribution (CC BY) license (<http://creativecommons.org/licenses/by/4.0/>).